

## Enhancing the performance of sustainable geopolymers: Insights into liquid-to-solid and alkali ratios

Moustafa Habib Chenafi <sup>\*,1,a</sup>, Zoubir Makhloufi <sup>1,2,b</sup>, Ahmed Othmane Bekkai <sup>1,c</sup>, Hichem Berkak <sup>3,d</sup>

<sup>1</sup>Structures Rehabilitation and Materials Laboratory (SREML), University Amar Telidji Laghouat, 03000, Algeria

<sup>2</sup>Civil Engineering Department, University Amar Telidji, Laghouat, 03000, Algeria

<sup>3</sup>Department of Structures and Materials, Faculty of Civil Engineering, University of Sciences and Technology Houari Boumediene (USTHB), Algiers, Algeria

### Article Info

#### Article History:

Received 22 Jan 2025

Accepted 06 Aug 2025

#### Keywords:

Geopolymer;  
Liquid-to-solid;  
Sodium silicate;  
Sodium hydroxide;  
Alkali ratios;  
Amorphous gels

### Abstract

This study investigates the impact of the liquid-to-solid (L/S) ratio and the sodium silicate-to-sodium hydroxide (SS/SH) ratio on the microstructural, physical, and mechanical properties of metakaolin-based geopolymer mortars. Sodium hydroxide (NaOH) and sodium silicate (Na<sub>2</sub>SiO<sub>3</sub>) were employed as alkaline activators, with the NaOH concentration fixed at 16 M. The SS/SH ratio ranged from 1 to 3, while L/S ratios of 0.5 to 0.8 were evaluated. The geopolymer samples were cured and analyzed after 28 days of aging. The study employed a range of advanced characterization techniques, including bulk density measurement, total porosity evaluation, mechanical properties testing, scanning electron microscopy (SEM), and X-ray diffraction (XRD). The findings revealed that the maximum compressive strength of 22.46 MPa was achieved at the optimal liquid-to-solid (L/S) ratio of 0.7 and sodium silicate-to-sodium hydroxide (SS/SH) ratio of 2.0. Microstructural analysis via SEM highlighted a dense and cohesive geopolymer matrix at this ratio, signifying improved mechanical performance. Additionally, phase analysis using XRD identified the presence of amorphous gels alongside crystalline zeolite phases, indicative of an amorphous structure formation that contributes to enhanced mechanical strength and structural integrity.

© 2025 MIM Research Group. All rights reserved.

## 1. Introduction

Inorganic aluminosilicate materials are known as geopolymers, which are produced by combining reactive aluminosilicate materials with potent alkaline activators [1]. Geopolymer's resource consumption, energy consumption, and CO<sub>2</sub> emissions are significantly lower than those of ordinary portland cement. The carbon emissions of 1 m<sup>3</sup> of geopolymer concrete are only 10% of those of concrete made with ordinary cement [2]. In general, geopolymers are a three-dimensional network structure that is composed of tetrahedral structure units of AlO<sub>4</sub> and SiO<sub>4</sub>. This concept was first introduced by Davidovits in the early 1970s [3]. Aluminosilicate activation by alkali is best understood as a two-part process: first, a liquid with a high alkali concentration; second, a solid with the right ratio of highly reactive silicate to aluminate [4]. The ratios of liquid to solid (L/S) and sodium silicate-to-sodium hydroxide (Na<sub>2</sub>SiO<sub>3</sub>/NaOH) significantly influence the physical and mechanical strength of geopolymers [5]. Sodium hydroxide (NaOH) and waterglass (Na<sub>2</sub>SiO<sub>3</sub>) are the two components that make up the activating solution that is used the most often. Xu et al. found that aluminosilicate particles were more thoroughly dissolved after activation with NaOH than with

\*Corresponding author: [mu.chenafi@univ-lagh.dz](mailto:mu.chenafi@univ-lagh.dz)

<sup>a</sup>orcid.org/ 0009-0000-8685-3570; <sup>b</sup>orcid.org/ 0000-0002-9175-9949; <sup>c</sup>orcid.org/0000-0003-2913-9172;

<sup>d</sup>orcid.org/0000-0002-0578-4815

DOI: <http://dx.doi.org/10.17515/resm2025-635ma0122rs>

Res. Eng. Struct. Mat. Vol. x Iss. x (xxxx) xx-xx

KOH [6]. The increased ability of NaOH to facilitate the liberation of aluminate and silicate monomers is responsible for this [7,8].

Yao et al. [9] indicated that a low liquid-to-solid (L/S) ratio, which pertains to the ratio of activator solution to aluminosilicate, leads to reduced slurry viscosity, whereas elevated L/S ratios prolong the geopolymerization duration. In contrast, Zuhua et al. [10], asserted that high L/S ratios could expedite the dissolution of source materials; however, they were not advantageous to the polycondensation process at high sodium hydroxide (NaOH) concentrations. Provis et al. [11] noted that geopolymers with extremely low L/S ratios typically fail to attain high strength as a result of the limited extent of binder formation. Jaya et al. [12] examined the effects of several L/S ratios, 1.66, 1.42, 1.25, 1.11, and 1, on the characteristics of MK850-based geopolymers. The experiment used an SS/SH ratio of 1 and a 10M NaOH solution. Following 28 days of maturation, the specimens attained an ideal compressive strength of 32 MPa with a liquid-to-solid ratio of 0.8.

Mohammed and Géber [13] investigated the hardening of the MK750-based geopolymer at 60°C and room temperature. They employed varying L/S ratios to many levels including 0.8, 0.95, and 1.1, and maintained a fixed SS/SH ratio at 1. The geopolymer achieved solidification at L/S ratio of 0.8 at ambient temperature, yielding a bulk density of 1.264 g.cm<sup>-3</sup> and a compressive strength of 19.12 MPa. The impact of the L/S ratio (0.7, 0.8, 1.0, and 1.25) and the proportions of Na<sub>2</sub>SiO<sub>3</sub>/NaOH (0.5, 1.0, 1.5, 2.0, and 2.5) on the preparation of metakaolin inorganic membrane geopolymer is the subject of a study by Ibrahim et al. [14]. The density reached its highest value at an SS/SH ratio of 2.5 and an L/S ratio of 0.7. Similarly, the lowest water absorption was observed at the same SS/SH ratio of 2.5 and L/S ratio of 0.7.

A study by Nur et al. [15] examines the impact of varying SS/SH ratios (0.4-1.2) on the microstructural, mechanical and physical characteristics of MK850-based geopolymer. By maintaining an SS/SH ratio of 1.0, the compressive strength reached its highest value of 32 MPa. Conversely, the material's strength diminished as the ratio exceeded 1.0, which was due to the excess alkali content. A more dense and compact structure was achieved as the outcome of the raised quantity of Na<sub>2</sub>SiO<sub>3</sub>, which contributed to the overall material strength.

In contrast, Hardjito and Rangan concluded that compressive strength rises as the Na<sub>2</sub>SiO<sub>3</sub>/NaOH ratio improves. Na<sub>2</sub>SiO<sub>3</sub>/NaOH ratios of approximately 2.5 were recommended for geopolymers derived from fly ash. For geopolymers derived from calcined kaolin, Wang et al. found a Na<sub>2</sub>SiO<sub>3</sub>/NaOH mass ratio of 0.24 [16]. Based on a variety of studies, waterglass facilitates the polymerization process, resulting in a reaction product with a higher mechanical strength and a higher concentration of silicon [17]. The combination should maintain its strength and workability by using a low Na<sub>2</sub>SiO<sub>3</sub>/NaOH ratio, according to Sathonsaowaphak et al.

In earlier studies, researchers primarily focused on utilizing fly ash as the primary aluminosilicate source for geopolymer production [18]. Subsequently, the focus shifted toward exploring combined aluminosilicate sources, such as fly ash and slag, which became prominent areas of research [19]. However, the direct use of raw metakaolin as a standalone precursor in geopolymer synthesis has not been extensively investigated [20]. Understanding the role of metakaolin as a fundamental material in geopolymer production is crucial to assess its capacity to function independently without supplementary materials. Furthermore, employing a single, well-defined material like metakaolin simplifies the interpretation of results by avoiding the complexities introduced by mixed or impure raw materials, such as fly ash, which often contains various impurities that can complicate data analysis [5].

In this investigation, we examined the effects of various L/S ratios and Na<sub>2</sub>SiO<sub>3</sub> ratios on the microstructure, physical and mechanical characteristics of MK750-based geopolymer mortars using NaOH mixed with a Na<sub>2</sub>SiO<sub>3</sub> solution (waterglass) as the major activator, following the background information given.

## 2. Materials and Experimental Procedures

### 2.1 Materials

Kaolin powder (KT) employed in this study was acquired from SAOLKA company Jijel Algeria. The present kaolin was ground to obtain 90 % of particles that measure  $<60 \mu\text{m}$ . the chemical composition of the kaolin as 65.11 %  $\text{SiO}_2$ , 23.07 %  $\text{Al}_2\text{O}_3$ , 3.29 %  $\text{K}_2\text{O}$ , 1.03 %  $\text{Fe}_2\text{O}_3$ , 0.31 %  $\text{Na}_2\text{O}$ , 1.32 %  $\text{CaO}$ , and 0.36 %  $\text{MgO}$  (on a mass basis), which his mineralogical composition, consists of 18% kaolinite, 44% quartz, 20% mica, and 18% orthoclase. To prepare the metakaolin (MK750), the natural kaolin was heated at  $750^\circ\text{C}$  in blast furnace static for 5 h. This thermal treatment process transformed the kaolin into metakaolin (MK750), which was then used as the precursor material for the geopolymer synthesis. Chemical compositions are determined by X-ray fluorescence analysis (XRF) of MK750 is given in Table 1.

Table 1. Chemical analysis of MK750 by (wt%)

	CaO	SiO <sub>2</sub>	Al <sub>2</sub> O <sub>3</sub>	Na <sub>2</sub> O	K <sub>2</sub> O	MgO	Fe <sub>2</sub> O <sub>3</sub>	LiO
MK750	1.09	70.23	22.25	0.31	3.95	0.32	1.28	0.57

The physical characterization of kaolin and its thermally activated form (MK750) revealed significant changes in surface and structural properties while maintaining a largely similar chemical composition. The BET surface area increased from  $7.16 \text{ m}^2/\text{g}$  for raw kaolin to  $12.43 \text{ m}^2/\text{g}$  for MK750, indicating enhanced surface reactivity due to the dehydroxylation process during calcination. True density showed a slight increase from  $2.73 \text{ g/cm}^3$  to  $2.77 \text{ g/cm}^3$ , and the  $\text{SiO}_2/\text{Al}_2\text{O}_3$  molar ratio rose from 2.82 to 3.15, reflecting subtle modifications in the silica-to-alumina balance. A substantial reduction in the loss on ignition (from 5.55% in kaolin to 0.57% in MK750) confirmed the effective removal of structural water and the successful transformation of crystalline kaolinite into an amorphous, highly reactive metakaolin phase. Moreover, particle size distribution analysis showed that only 5.6% of the MK750 particles were retained on a  $60 \mu\text{m}$  sieve, indicating that 94.4% passed through, which demonstrates the fine and homogeneous nature of the calcined material. Such a fine particle structure is particularly desirable for geopolymer applications, as it promotes better dissolution in alkaline solutions and enhances the compactness and mechanical performance of the final matrix.

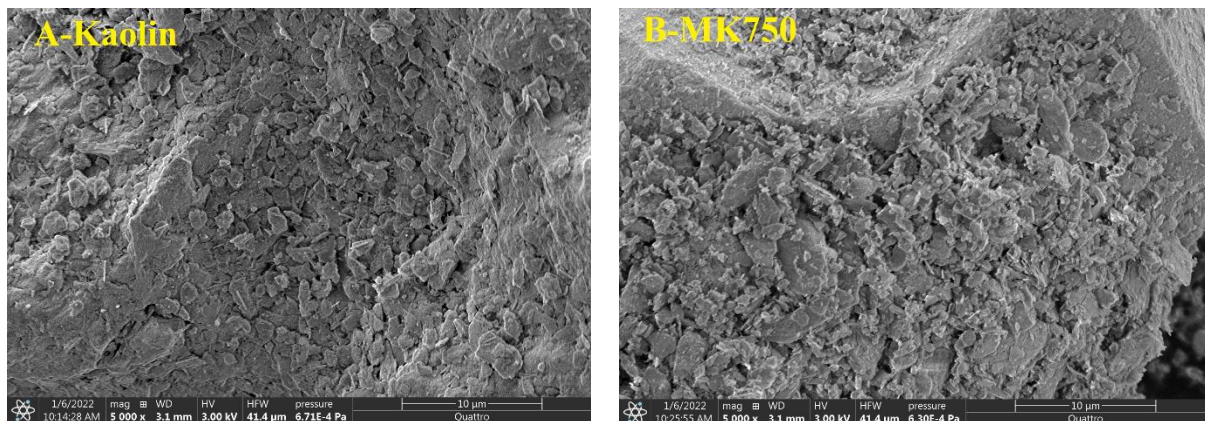


Fig. 1. SEM images of (A) Kaolin (KT) and (B) Metakaolin (MK750)

The morphological characteristics are also significantly affected by the calcination process. As shown in Figure 1, the kaolin sample (Fig. 1-A) exhibits a typical plate-like morphology, which corresponds to the layered crystal structure of kaolinite. After thermal treatment, MK750 particles (Fig. 1-B) lose this plate-like shape and adopt more irregular and in some cases spherical forms, with a more homogeneous and reduced particle size. These morphological changes can be attributed to the dehydroxylation of kaolinite and the collapse of its crystalline structure during calcination, contributing further to the increased reactivity of the metakaolin.

The alkaline solution utilized in this study was prepared by combining sodium hydroxide (NaOH) and sodium silicate (Na<sub>2</sub>SiO<sub>3</sub>) solutions. The sodium hydroxide was obtained as micro-pears of caustic soda with a purity of 99%, supplied by FAPROCO-CHIM, Algeria. The sodium silicate solution, procured from GALAXY-CHIMIE, M'sila, Algeria, contained 26% SiO<sub>2</sub>, 13% Na<sub>2</sub>O, and 61% H<sub>2</sub>O. The sodium silicate solution exhibited a SiO<sub>2</sub>/Na<sub>2</sub>O modulus of 2, which is ideal for promoting effective geopolymerization.

## 2.2 Experimental Procedures

### 2.2.1 Sample's Preparation

The mixing procedure and formulation of the geopolymer mortar were based on the principles outlined in Joseph Davidovits' book *Geopolymer Chemistry and Applications*, specifically in the chapter titled "How to quantify and develop formulas" [21], as illustrated in Fig. 2. To ensure reproducibility, a 16M NaOH liquid was prepared and mixed with Na<sub>2</sub>SiO<sub>3</sub>, with the SS/SH ratio adjusted between 1 and 3 depending on the mix design. The specifics of the mixing parameters are comprehensively outlined in Table 2. The metakaolin (MK750) was gradually added to the prepared alkaline solution to prevent clumping and ensure uniform dispersion (Fig. 2-A). The sand, being an inert material, was added after the reactive components were fully mixed, and the mixture was homogenized again for 3-5 minutes to ensure proper consistency.

The mixture was then transferred to prismatic molds, and air bubbles were removed using mechanical vibration for 30 seconds. The samples underwent curing in a controlled atmosphere at 65°C for 24 hours, with molds protected by plastic film to avoid moisture loss and carbonation (Fig. 2-B). After demolding, the specimens were stored at ambient temperature (25 ± 2 °C, 60 ± 5% RH) for 28 days to complete the curing process (Fig. 2-C) [22]. The mortars under investigation were subjected to three-point bending tests after a 28-day curing period. Subsequently, the samples obtained during the bending test were compressed (Fig. 2-D).

Table 2. Mix design of metakaolin based geopolymer mortars.

L/S	SS/SH	Liquid (g)	MK (g)	Sand (g)	SS (g)	SH (g)
0.5	1	225	450	1350	112.5	112.5
	1.5				135	90
	2				150	75
	2.5				160.71	64.28
	3				168.75	56.25
0.6	1	270	450	1350	135	135
	1.5				162	108
	2				180	90
	2.5				192.85	77.14
	3				202.5	67.5
0.7	1	315	450	1350	157.5	157.5
	1.5				189	126
	2				210	105
	2.5				225	90
	3				236.25	78.75
0.8	1	360	450	1350	180	180
	1.5				216	144
	2				240	120
	2.5				257.14	102.85
	3				270	90



**A- The reactive components were fully mixed.**



**B- To avoid moisture loss and carbonation, the molds were covered with plastic film, and the samples were cured at 65°C for 24 hours.**



**C-Post-demolding, specimens were kept at  $25 \pm 2^\circ\text{C}$ ,  $60 \pm 5\%$  RH for 28 days to complete curing.**



**D-Three-point bending and uniaxial compressive experiments of geopolymer mortar after 28 days.**



Fig. 2. Images illustrate the preparation and testing of geopolymer mortar (GPM)

### 2.2.2 Characterization methods

Archimedes' principle (EN 993-1) was employed to determine the bulk densities of the samples, and the average of five determinations for each sample is reported. The true density of the samples was ascertained using the helium pycnometer method (Multipycnometer, Quantachrome). The total porosity of the GPMs was determined using the following Eq (1):

$$\text{Total porosity (\%)} = \left(1 - \frac{\text{bulk density}}{\text{true density}}\right) \times 100 \quad (1)$$

The mortars under study were subjected to three-point bending tests in accordance with EN 196-1 in order to measure their flexural strength (Fig 3). The "CONTROLS" press, which has a loading rate of 50 N/s and a maximum load of 100 kN, was used to test three prismatic samples ( $4 \times 4 \times 16 \text{ cm}^3$ ) for each composition. A conventional formula Eq (2) was used to determine the flexural strength after samples were loaded at the midway and sustained at both ends till failure.

$$\delta_F = \frac{3F_f l}{2b^3} \quad (2)$$

Where,  $\delta_F$ : Flexural strength,  $F_f$ : Applied load at the point of failure (N),  $l$ : Length of the support span (cm or mm),  $b$ : Width of the sample (cm or mm).

The six samples taken during the bending test were compressed on a  $4 \times 4 \text{ cm}^2$  piece of material (Fig 3) by formula Eq (3) in accordance with European standard EN 196-1. After 28 days, both tests were carried out.

$$\delta_c = \frac{F_c}{b^2} \quad (3)$$

Where,  $\delta_c$ : Compressive strength,  $F_c$ : Applied load at the point of failure (N),  $b$ : Width of the sample (cm or mm).

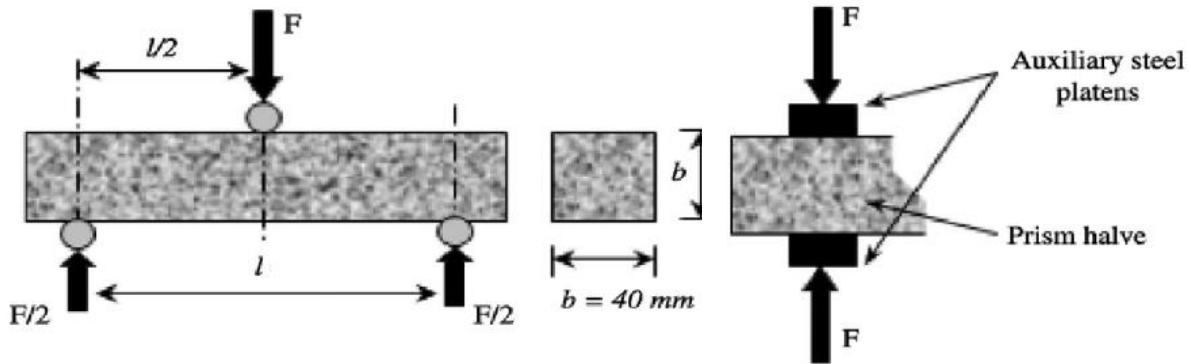


Fig. 3. Three-point bending and uniaxial compression tests

The X-ray diffraction of the unprocessed material and the optimized sample was conducted using Cu  $K\alpha$  radiation (Philips-PW3170 diffractometer) to determine the crystalline phases or amorphous property. The microstructure of the samples was examined using a VEGA3 TESCAN type scanning electron microscopy.

### 3. Result and discussion

#### 3.1 Bulk Density

The correlation among bulk density, the liquid-to-solid ratio (L/S), and the sodium silicate-to-sodium hydroxide ratio (SS/SH) was examined in accordance with Figure 4. The findings indicate a distinct trend in which both L/S and SS/SH ratios substantially affect the bulk density of the geopolymer material.

As the L/S ratio increases, the density of the MK750-based geopolymer consistently rises across all SS/SH ratios. For  $L/S = 0.5$ , the density rises by 3.98% from SS/SH ratio 1 to 1.5, with the density increasing from  $1.783 \text{ g/cm}^3$  to  $1.854 \text{ g/cm}^3$  and then continues to grow, reaching a 3.13% increase at SS/SH ratio 2, where the density becomes  $1.912 \text{ g/cm}^3$ . This is followed by a 2.35% increase at SS/SH ratio 2.5 and a 1.64% drop at SS/SH ratio 3 ( $1.989 \text{ g/cm}^3$ ). At  $L/S = 0.6$ , the rise from SS/SH ratio 1 to 1.5 is 2.69%, where the density increases from  $2.042 \text{ g/cm}^3$  to  $2.097 \text{ g/cm}^3$ , then 2.00% at SS/SH ratio 2, 1.36% at SS/SH ratio 2.5, and 0.69% at SS/SH ratio 3, where the density reaches

2.183 g/cm<sup>3</sup>. This increase can be attributed to improved distribution and mixing of the components, resulting in a more homogeneous structure and compact matrix [23]. An increase in liquid content tends to facilitate better particle dispersion and compaction of the material, effectively reducing internal void spaces and enhancing overall bulk density [13,20]. In parallel, the content of sodium oxide (Na<sub>2</sub>O), derived from the alkaline activators, performs a critical function in the polymerization reaction. An excess of Na<sub>2</sub>O improves the solubility of the aluminosilicate source "MK750" and facilitates the release of Si<sup>4+</sup> and Al<sup>3+</sup> ions, thereby promoting more extensive gel formation [10]. This contributes to the densification of the geopolymer structure and further supports the observed increase in density at elevated liquid to solid ratios [24].

For L/S = 0.7, the rise from SS/SH ratio 1 to 1.5 is 1.77%, where the density increases from 2.205 g/cm<sup>3</sup> to 2.244 g/cm<sup>3</sup>, followed by a 1.11% increase at SS/SH ratio 2 (2.269 g/cm<sup>3</sup>), a 0.53% increase at SS/SH ratio 2.5, leads to a density of 2.281 g/cm<sup>3</sup>, and a little decrease of 0.04% at SS/SH ratio 3, where the density remains almost the same at 2.280 g/cm<sup>3</sup>, may indicate a saturation point of sodium silicate contribution. This trend is remarked upon by Bowen et al. and Shoaee et al. [25,26], owing to the higher concentration of sodium silicate (Na<sub>2</sub>SiO<sub>3</sub>), which promotes ion densification and improves the structural cohesion of the geopolymer. Sodium silicate (Na<sub>2</sub>SiO<sub>3</sub>) acts as a binder that reduces porosity by enhancing the gel phase formation N-A-S-H, leading to denser and more compact materials [27]. In present investigation, the density slightly decreased beyond an SS/SH ratio of 2.5 (e.g., from 2.281 g/cm<sup>3</sup> at SS/SH = 2.5 to 2.280 g/cm<sup>3</sup> at SS/SH = 3 for L/S = 0.7, and from 2.298 to 2.281 g/cm<sup>3</sup> for L/S = 0.8), supporting the interpretation that excessive sodium silicate content may lead to a viscosity increase and reaction inefficiency, thus limiting further densification of the geopolymer matrix. Similarly, these findings are consistent with the results reported by Kwek et al. and Jaya et al., who observed a slight decrease in density at higher SS/SH ratios in alkali-activated geopolymers. In their studies, this phenomenon was attributed to the slowdown of the geopolymerization process in later stages, as well as water loss due to evaporation during the reaction [28,29].

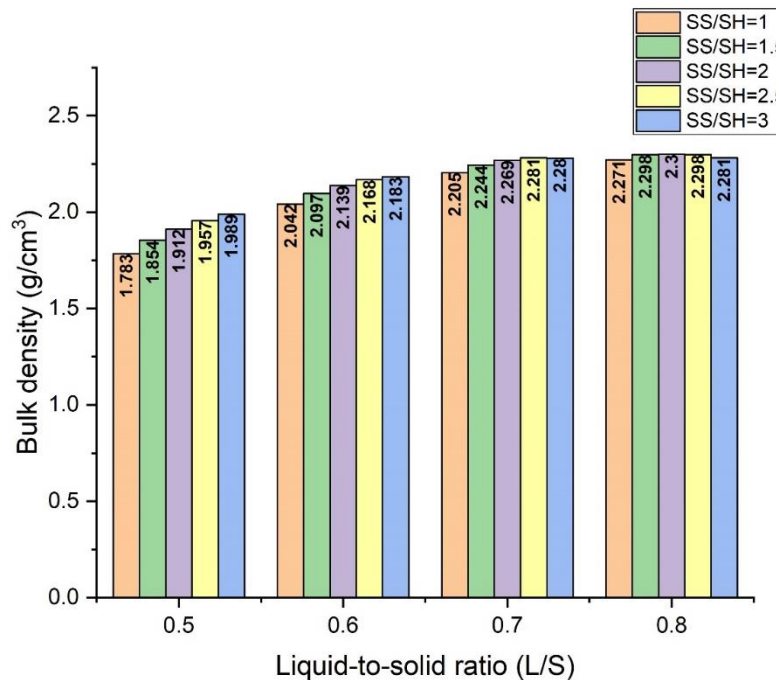


Fig. 4. bulk density of metakaolin-based geopolymer mortar with different L/S and SS/SH ratios

However, at L/S = 0.8, the rise from SS/SH ratio 1 to 1.5 is 1.19%, where the density increases from 2.271 g/cm<sup>3</sup> to 2.298 g/cm<sup>3</sup>. With a 0.09% gain at SS/SH ratio 2 (2.300 g/cm<sup>3</sup>), a 0.09% drop at SS/SH ratio 2.5, resulting in a density of 2.298 g/cm<sup>3</sup>, and a 0.74% decline at SS/SH ratio 3, where the density drops to 2.281 g/cm<sup>3</sup>. An oversaturated geopolymer system may result from an excessively high L/S ratio, which could potentially impair the formed structure despite the rise in density. This oversaturation can be ascribed to the surplus Na content in the geopolymer system

[13,25]. The geopolymerization process may be impeded and the density of the resultant geopolymer may be compromised as the SS/SH ratio rises.

### 3.2 Total Porosity

Figure 5 show the total porosity of MK750-based geopolymer mortar with different L/S and SS/SH ratios. Porosity decreases as the L/S ratio increases for all SS/SH values.

Total porosity typically declines with raise in the SS/SH ratio, particularly at lower L/S ratios. At an L/S ratio of 0.5, porosity exhibits an 11.5% reduction as the SS/SH ratio rises from 1 to 1.5, decreasing from 25.71% to 22.75%. This trend continues with a further decline to 20.33% at an SS/SH ratio of 2, representing a 10.6% decrease. The porosity then decreases to 18.46% at an SS/SH ratio of 2.5, indicating a 9.2% reduction, and ultimately falls to 17.13% at an SS/SH ratio of 3, corresponding to a 7.2% decrease. At L/S = 0.6, porosity decreases by 15.4% as the SS/SH ratio rises from 1 to 1.5, changing from 14.92% to 12.63%. It further declines to 10.88% at an SS/SH ratio of 2, representing a 13.9% decrease, and continues to 9.67% at an SS/SH ratio of 2.5, indicating an 11.1% decrease. Finally, it drops to 9.04% at an SS/SH ratio of 3, reflecting a 6.5% decrease. At an L/S ratio of 0.7, porosity exhibits a decrease of 19.9% as the SS/SH ratio rises from 1 to 1.5, transitioning from 8.12% to 6.5%. Subsequently, it further declines to 5.46% at an SS/SH ratio of 2, representing a 16.0% reduction, and then experiences a minor decrease to 4.96% at an SS/SH ratio of 2.5, corresponding to a 9.2% reduction. At an SS/SH ratio of 3, a marginal rise of 0.8% is noted, with porosity rising to 5%. Higher SS/SH ratios correspond to increased sodium silicate content, which enhances gel formation, fills the pores, and leads to a denser microstructure with reduced porosity [30].

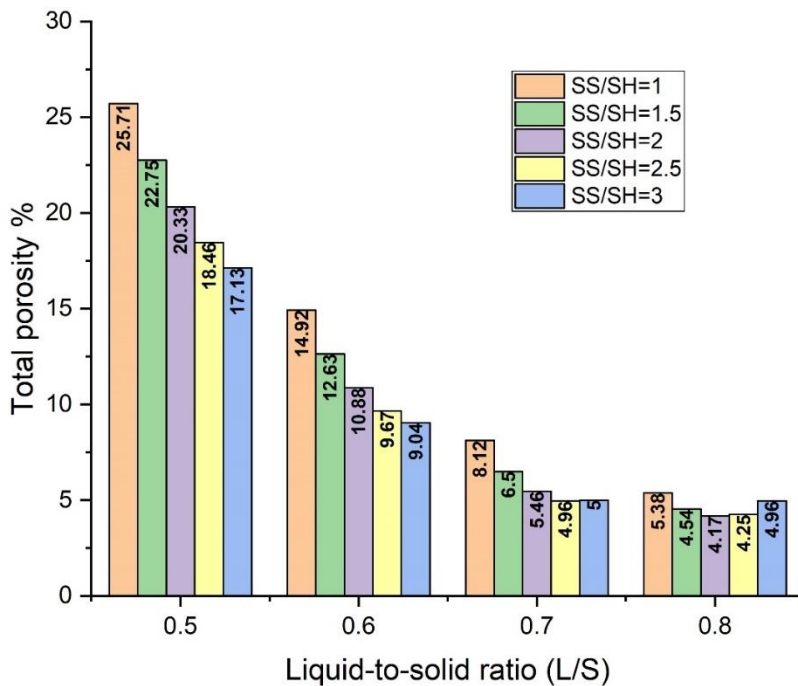


Fig. 5. Total porosity of metakaolin-based geopolymer mortar with different L/S and SS/SH ratios.

At an L/S ratio of 0.8, porosity decreases by 15.6% as the SS/SH ratio increases from 1 to 1.5, changing from 5.38% to 4.54%. This trend continues, with a further decrease to 4.17% at an SS/SH ratio of 2, representing an 8.1% reduction. These values indicate the lowest porosity observed, indicating a stronger influence of sodium silicate on reducing porosity. During the geopolymerization process, MK750 significantly contributes to the reduction of porosity. by enhancing the generation of polymeric gels that tightly bond the particles together. This aligns with the results of Zhou et al. [31], who highlighted the importance of alkali activators in dissolving the aluminosilicate source (MK). Additionally, Ibrahim et al. highlighted that the mechanical properties of the geopolymer are enhance and, and its porosity is further reduced due to the formation of Si-



O-Si bonds, which demonstrate superior strength relative to Si-O-Al bonds, owing to the increased SiO<sub>2</sub> content [32].

A 1.9% increase in porosity is observed at an SS/SH ratio of 2.5, raising it to 4.25%. At an SS/SH ratio of 3, porosity increases by 16.7%, reaching 4.96%. Total porosity starts to stabilize or slightly increase in total porosity for SS/SH ratio more than 2, likely due to excessive the alkaline activator causing reduced cohesion [27]. further increases in Na<sub>2</sub>O content destabilize oligomeric silicate species, shifting the equilibrium towards the formation of mononuclear silicate species SiO<sub>2</sub>(OH)<sub>2</sub><sup>2-</sup> and SiO(OH)<sub>3</sub><sup>-</sup> and generating excess hydroxide ions (OH<sup>-</sup>). Ultimately, the polycondensation process is rendered less effective by the presence of these excess hydroxide ions, which results in an increase in total porosity [33].

### 3.3 Compressive Strength

Compressive strength ( $C_{s28}$ ) rises with an increase in the L/S ratio for most SS/SH ratios, as indicated in figure 6. The compressive strength typically increases with rising SS/SH ratios, peaking at the second increment (SS/SH = 2), particularly at lower L/S ratios. At an L/S ratio of 0.5, the compressive strength exhibits an increase of 121.51%, rising from 5.44 MPa at SS/SH ratio 1 to 12.05 MPa at SS/SH ratio 2. However, it subsequently decreases by 18.84%, falling from 12.05 MPa at SS/SH ratio 2 to 9.78 MPa at SS/SH ratio 3. At L/S = 0.6, a 28.18% increase is noted from the SS/SH ratio of 1 (13.59 MPa) to the SS/SH ratio of 1.5 (17.42 MPa), followed by a decrease of 10.51% at the SS/SH ratio of 3 (15.59 MPa). At L/S = 0.7, the compressive strength exhibits an increase of 17.70% from an SS/SH ratio of 1 (18.19 MPa) to an SS/SH ratio of 1.5 (21.41 MPa). However, there is a notable decrease of 16.04% from an SS/SH ratio of 2.5 (21.26 MPa) to an SS/SH ratio of 3 (17.85 MPa). For L/S = 0.8, the increase from SS/SH ratio 1 (13.23 MPa) to SS/SH ratio 1.5 (21.89 MPa) is 65.46%, followed by a decrease of 24.44% at SS/SH ratio 3 (16.54 MPa).

The rising in strength is due to improved workability and better distribution of components at higher L/S ratios, resulting in improved structural integrity [20]. As a liquid content increases, results in augmentation of the Na<sub>2</sub>O content, leaching of silica and alumina from the source materials (MK750) is enhanced, leading to the formation of more polymeric networks and a consequent increase in compressive strength. However, at very high L/S ratios (e.g., 0.8), compressive strength starts to stabilize or slightly decrease for some SS/SH ratios, likely due to excessive liquid content causing reduced cohesion [27].

At each L/S ratio, compressive strength rises with higher SS/SH ratios up to around 2.0. Higher sodium silicate content promotes stronger gel formation, enhancing structural cohesion and mechanical strength [34,35]. The mixture's silica content is enhanced as the Na<sub>2</sub>SiO<sub>3</sub>/NaOH ratio increases. The kinetics of the geopolymerization reaction and the promotion of the formation of NASH gel are directly influenced by the presence of soluble silica, which is advantageous for the development of strength [32,36]. Beyond SS/SH = 2.5, compressive strength either stabilizes or slightly decreases due to reduced reactivity and possible oversaturation of activators [37]. A higher concentration of silicate in the system is responsible for the decrease in compressive strengths as the Na<sub>2</sub>SiO<sub>3</sub>/NaOH ratio increases. This is because an excessive amount of Na<sub>2</sub>SiO<sub>3</sub> impedes the evaporation of water and the formation of the structure [38]. This outcome aligns with the results of Moutaoukil et al [36] and Mustafa Al Bakri et al [39].

It is important to highlight that similar L/S ratios cannot be attained for both fly ash and MK-geopolymers due to differences in workability. Metakaolin exhibits a greater aqueous demand compared to fly ash, primarily because of the variations in particle morphology; metakaolin has a layered structure, whereas fly ash particles are spherical, resulting in lower water requirements for fly ash-based systems [40]. Kong et al. and Yong-Sing et al. [23,41] indicated that the higher liquid-to-solid ratios for MK-based geopolymers and FA-based geopolymers are 1.25 and 0.33, respectively. The strength of the final product is closely related to the void volume and porosity of the material, which are the direct result of the geopolymer paste's workability limitations [42].

As demonstrated by Joanna Marczyk et al. [43], the optimal L/S ratio is contingent upon the antecedent material's composition (fly ash or metakaolin); nevertheless, a lesser L/S ratio, approximately 0.30, was determined to be the most favorable for attaining a higher compressive

strength. In the research undertaken by Maheswaran et al. [44], the compressive strength of the geopolymer was enhanced from 27.75 MPa to 45 MPa by substituting with slag and fly ash. However, the workability was diminished as a consequence. Additionally, the introduction of industrial byproducts, such as slag, rice husk ash (RHA), fly ash, and nano-silica (NS), significantly enhanced the effectiveness of geopolymer concrete, so positioning it as a viable and ecologically friendly substitute for typical Portland cement concrete.

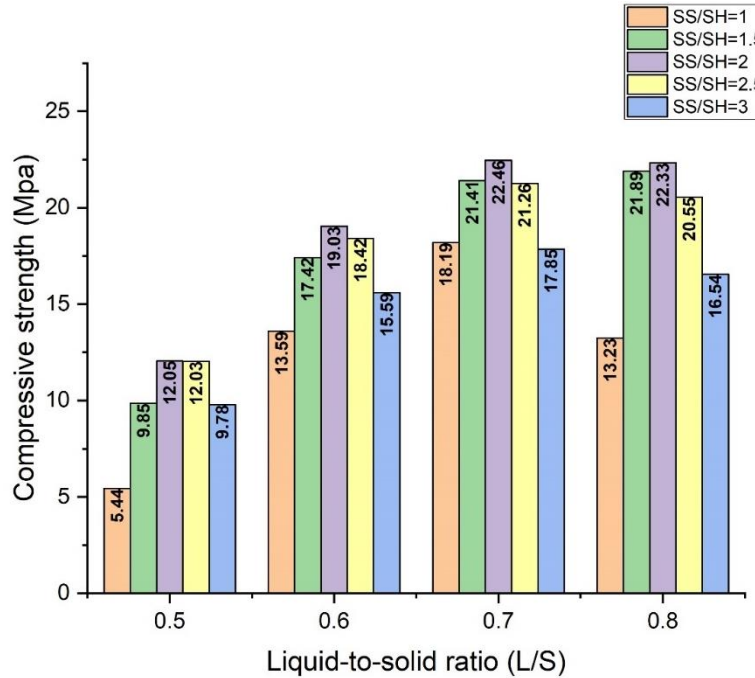


Fig. 6. compressive strength of metakaolin-based geopolymer mortar with different L/S and SS/SH ratios.

According to Chen et al. [3], As the L/S ratio grew, the compressive strength declined, as evidenced by the "Coal Gasification Slag-Based" study. An L/S ratio of 0.25 yielded the maximum compressive strength of 48.31 MPa, whereas an L/S ratio of 0.45 produced the minimum compressive strength of 2.41 MPa. Concurrently, the porosity of the material increased as the L/S ratio increased. The microstructure was denser at L/S = 0.25, as evidenced by the lowest total porosity of 1.45%. Conversely, the structural integrity was compromised and cavity formation was increased as the L/S ratio raised. According to the findings of Maheswaran et al [45], the split tensile and compressive strengths of geopolymer are enhanced by an increase in the slag content, despite the fact that workability is diminished. Using a constant binding agent concentration of 550 kg/m<sup>3</sup> and an alkaline solution ratio of 1 to 2.5, the optimal performance was attained with a 70:30 FA:GGBS ratio, a 13 M NaOH concentration, and an L/S ratio of 0.55. In summary, MK750-based geopolymers exhibit increased compressive strength, with studies indicating an enhancement to 45 MPa through the incorporation of slag and fly ash. Fly ash and GGBS demonstrate cost-effectiveness and offer comparable performance with enhanced workability, whereas RHA presents greater variability. The selection of material is contingent upon the particular application, necessitating a balance among performance, cost, and environmental impact.

### 3.4 Flexural Strength

Figure 7 showed flexural strength of metakaolin-based geopolymer mortar with different L/S and SS/SH ratios. Flexural strength ( $F_{s28}$ ) increases consistently as the **L/S ratio** rises, regardless of the SS/SH ratio. The flexural strength exhibits a rise with elevated SS/SH ratios; however, the rate of rise diminishes at higher SS/SH ratios. For L/S = 0.5, the rise in the SS/SH ratio from 1 (3.97 MPa) to 1.5 (5.83 MPa) is 46.85%, followed by a decrease of 6.08% from the SS/SH ratio of 2.5 (6.41 MPa) to 3 (6.02 MPa). At L/S = 0.6, there is a 13.72% rise from the SS/SH ratio of 1 (9.04 MPa) to 1.5 (10.28 MPa), followed by a decrease of 5.11% at the SS/SH ratio of 3 (10.39 MPa). At an L/S ratio

of 0.7, the flexural strength exhibits a rise of 8.68% from an SS/SH ratio of 1 (12.21 MPa) to 1.5 (13.27 MPa), while a decrease of 20.09% is observed at an SS/SH ratio of 3 (10.86 MPa). For L/S = 0.8, the rise in the SS/SH ratio from 1 (13.47 MPa) to 1.5 (14.35 MPa) is 6.53%, followed by a decrease of 6.48% at an SS/SH ratio of 3 (13.42 MPa). The findings indicate that rise in the SS/SH ratio initially enhances flexural strength; however, further rises result in diminishing or adverse effects.

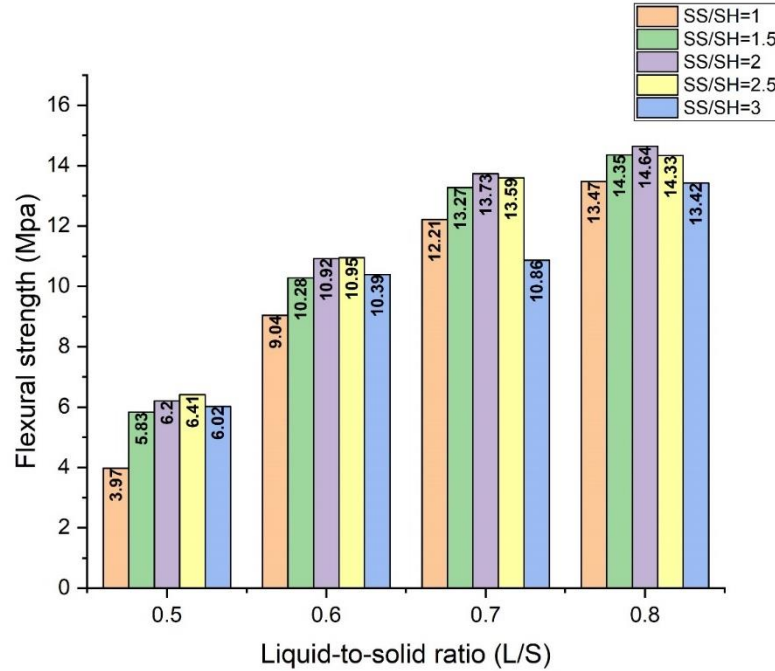


Fig. 7. Flexural strength of metakaolin-based geopolymer mortar with different L/S and SS/SH ratios

At lower L/S ratios, the material exhibits lower flexural strength due to insufficient liquid content, which hinders proper compaction and matrix formation [46]. Higher L/S ratios improve workability and enhance the bond between components, resulting in stronger flexural performance. Flexural strength improves with increasing SS/SH ratios, peaking around SS/SH = 2.0 and 2.5. Higher sodium silicate ( $\text{Na}_2\text{SiO}_3$ ) content enhances gel formation and structural cohesion, leading to better load distribution and higher flexural resistance [47]. At SS/SH = 3.0, the flexural strength shows a slight stabilization or reduction at high L/S ratios, likely due to oversaturation of activators affecting the matrix's homogeneity [48]. Thus, the phenomenon where compressive strength decreases and flexural strength increases at optimal L/S ratios is noted by Shilar et al. and Shoaie et al. [26,49], it can be generally explained by the interaction between the liquid content, compaction efficiency, and the chemical activation of the geopolymer. The reduction in compressive strength can be assigned to the excessive alkaline activator content, particularly  $\text{Na}_2\text{SiO}_3$ , which initially enhanced the dissolution of reactive particles. However, beyond a certain threshold, free and unreacted silicates accumulated, leading to the formation of irregular, weak gel structures. Additionally, the surplus liquid increased porosity, weakening the internal cohesion of the geopolymer matrix. Alkali frosting phenomena were also observed on the specimen surfaces, resulting in reduced network density and diminished compressive strength [49].

Conversely, the improvement in flexural strength due to enhanced workability from the higher liquid content, which promoted better stress distribution under flexural loading. Furthermore, the increased  $\text{SiO}_2/\text{Al}_2\text{O}_3$  ratio favored promoted to generate of more robust Si-O-Si bonds relative to Si-O-Al bonds, contributing to better bending resistance despite the higher porosity. Early-stage polymerization also produced partially flexible gel structures, supporting flexural strength even though the overall material density was reduced [50].

### 3.5 Microstructural Analysis Based on L/S Ratios

#### 3.5.1 SEM Analysis

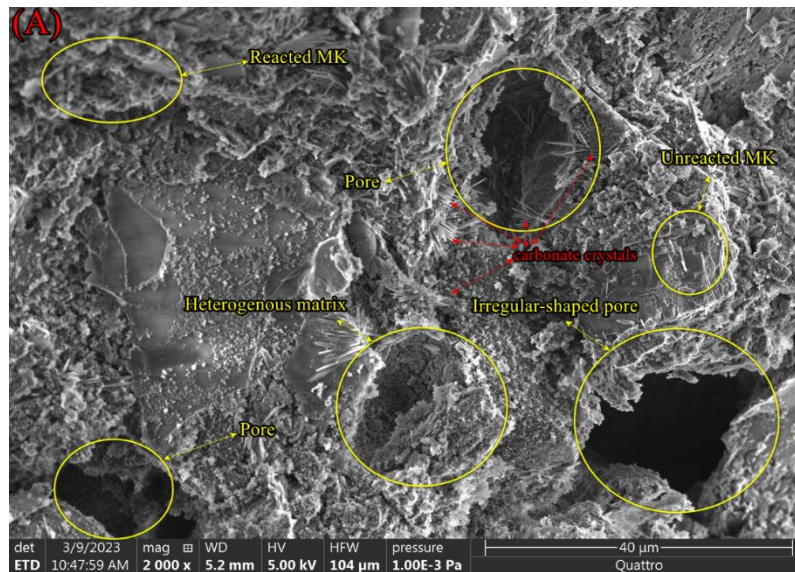
The microstructural behavior of geopolymer materials at varying liquid-to-solid (L/S) ratios reveals significant differences in the density, porosity, and overall mechanical properties of the material. The analysis at each ratio is described as follows:

Figure 8(A) presents the SEM results for a sample with an L/S ratio of 0.5. The microstructure exhibits high porosity with large voids due to insufficient liquid content to adequately activate the binder and fill the voids. A significant portion of the metakaolin particles remains unreacted, resulting in a weak and poorly connected geopolymer network. The bonds between particles are weak and lack cohesion, leading to poor compaction and low material density. In addition to the visible surface efflorescence, internal carbonation (sub-fluorescence) is also evident, with carbonate crystals forming within the pore network near the surface, as shown in Fig. 8 (A). These carbonate crystals can induce cracks and internal stresses in the porous matrix and pore network [51].

Figure 8(B) illustrates the SEM results for a sample with an L/S ratio of 0.6. The microstructure shows noticeable improvement, with reduced porosity and fewer voids compared to L/S = 0.5. More particles are chemically activated, forming a better-connected geopolymer network. However, some voids are still present due to slightly inadequate liquid content.

Figure 8(C) shows the SEM results for a sample with an L/S ratio of 0.7. The geopolymer matrix achieves a dense and well-connected network with significantly reduced porosity and a uniform structure. The bonds between the components are strong, and almost all metakaolin particles are fully reacted, contributing to a cohesive and robust material. Voids are minimized, leading to a compact microstructure. This morphology clearly displayed the amorphous geopolymer phase [52] which is in agreement with the XRD pattern.

Figure 8(D) presents the SEM results for a sample with an L/S ratio of 0.8. The microstructure becomes denser and more homogeneous, with further reductions in porosity compared to L/S = 0.7. Most particles are fully reacted, and the matrix is nearly void-free. Several needle-like structures were observed on the surface of the geopolymer binder in the SEM micrograph of sample. However, excessive liquid content may create thin films between particles, weakening the mechanical interlocking within the matrix. The slight over-saturation of liquid results in reduced cohesion and strength under compression.





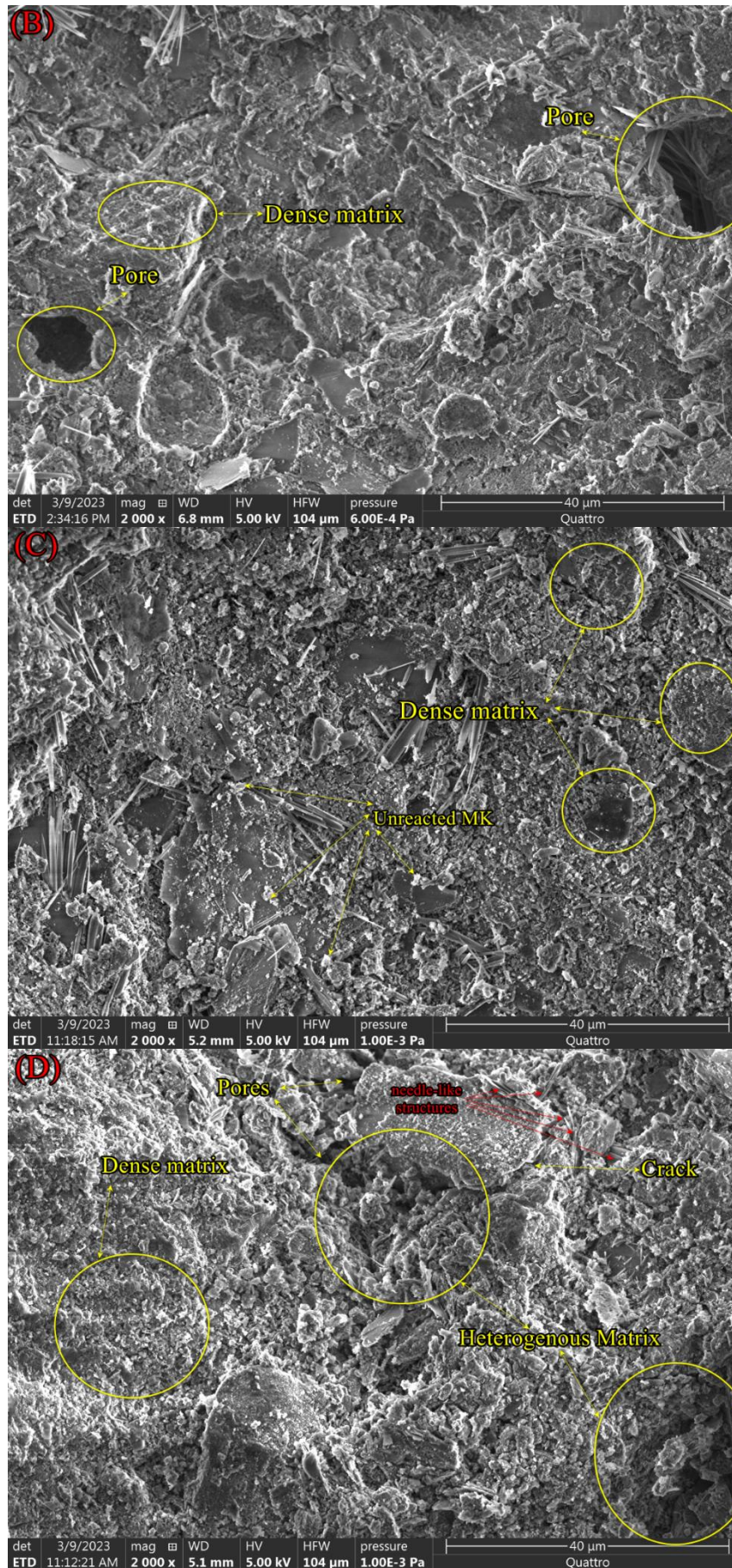


Fig. 8. SEM images of metakaolin based geopolymers with increasing L/S ratio of 0.5 (A), 0.6 (B), 0.7 (C), and 0.8 (D)

### 3.5.2 XRD Analysis

Figure 9 presents the XRD patterns of metakaolin and geopolymer mortars (GPMs) synthesized at various liquid-to-solid (L/S) ratios. To investigate the relationship between L/S ratios, compressive strength, and phase composition, GPM samples with the lowest (L/S = 0.5), medium (L/S = 0.7), and highest (L/S = 0.8) compressive strength values were analyzed for intensity variations. The XRD pattern of raw metakaolin exhibited characteristic diffraction peaks corresponding to quartz, muscovite, and orthoclase, which are indicative of its crystalline mineralogical composition. The GPMs synthesized at an L/S ratio of 0.8 exhibited characteristic peaks corresponding to zeolite, indicating a significant presence of crystalline zeolite [53]. This high zeolite content is associated with a relatively lower compressive strength of approximately 22.33 MPa compared to the sample with an L/S ratio of 0.7, as illustrated in Fig. 9. However, the GPMs synthesized at an L/S ratio of 0.7 displayed predominantly amorphous XRD patterns characterized by unclear hump within the range of  $2\theta = 20^\circ\text{--}40^\circ$ . This amorphous nature, though slightly influenced by impurities present in the MK750 precursor, aligns well with previously reported patterns of geopolymers, indicating effective geopolymerization [54]. Conversely, the GPMs synthesized at an L/S ratio of 0.5 exhibited the appearance of natron ( $\text{Na}_2\text{CO}_3 \cdot 10\text{H}_2\text{O}$ ), which is indicative of unreacted alkali components. The presence of natron adversely affected the physical and mechanical properties of the geopolymer, resulting in a less cohesive and mechanically inferior matrix [51]. This is corroborated by the results of the physical and chemical tests, as well as the SEM image analysis (Fig.8A).

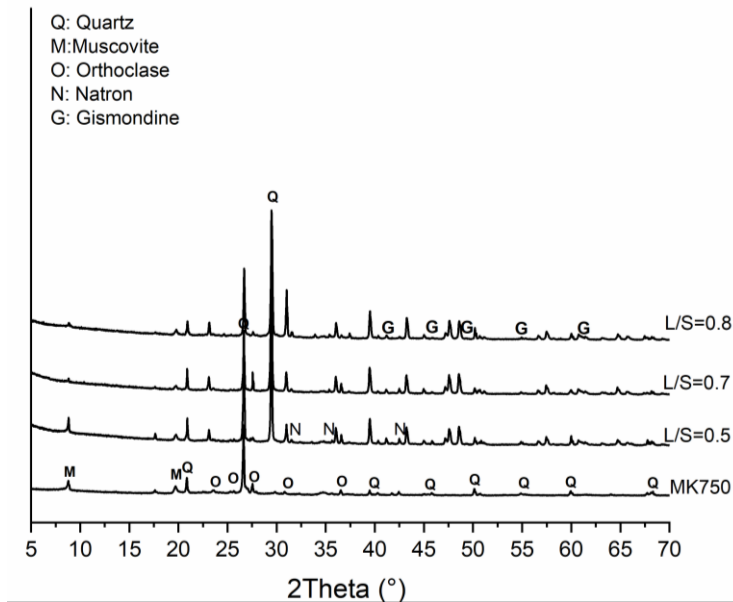


Fig. 9. XRD patterns of metakaolin and geopolymer mortars (GPMs) synthesized at various liquid-to-solid (L/S) ratios

## 4. Conclusions

This study investigated the influence of liquid-to-solid (L/S) and sodium silicate-to-sodium hydroxide (SS/SH) ratios on the microstructural, physical, and mechanical properties of MK750-based geopolymer mortars. The results demonstrated that increasing both L/S and SS/SH ratios improved the bulk density and reduced the porosity of the geopolymer mortars. The highest bulk density was observed at L/S = 0.7 and SS/SH = 2.5, while the lowest porosity occurred at the same L/S ratio and SS/SH ratio of 2.5. These findings confirm that an optimal balance between the L/S and SS/SH ratios is crucial for improving the geopolymer material's structural properties.

Regarding mechanical performance, the compressive strength peaked at 22.46 MPa at L/S = 0.7 and SS/SH = 2.0, while the greatest flexural strength was observed at L/S = 0.8. These results indicate that both compressive and flexural strength are significantly influenced by the interaction between the L/S and SS/SH ratios, with the optimal values for each ratio identified in this study.



Furthermore, the observed slight decrease in bulk density at  $L/S = 0.8$  and  $SS/SH = 3.0$ , compared to  $L/S = 0.7$  and  $SS/SH = 2.5$ , highlights the detrimental effect of excessive liquid or alkali content. This phenomenon can be attributed to the oversaturation of the geopolymer system, which may hinder the polymerization process and promote increased porosity due to water loss and insufficient gel formation.

Microstructural analysis, conducted using scanning electron microscopy (SEM), revealed that the geopolymer matrix became denser and more cohesive at higher  $L/S$  ratios, indicating improved mechanical performance. X-ray diffraction (XRD) analysis confirmed the dominance of an amorphous phase at  $L/S = 0.7$ , which was associated with the highest compressive strength. At  $L/S = 0.8$ , however, crystalline zeolite peaks were identified, which correlated with reduced mechanical strength.

Based on these findings, an  $L/S$  ratio of 0.7 and an  $SS/SH$  ratio between 2.0 and 2.5 are recommended for achieving the optimal mechanical and microstructural performance in geopolymer mortars. These optimal conditions ensure the best balance between density, porosity, and strength, making them highly suitable for applications in sustainable construction materials.

## References

- [1] Barzoki PK, Gowayed Y. Tailoring Metakaolin-Based Geopolymers for High-Temperature Stability: Chemical, Thermal & Mechanical Insights. *Ceram Int* 2025. <https://doi.org/10.1016/j.ceramint.2024.12.553>
- [2] Shi X, Zhang C, Wang X, Zhang T, Wang Q. Response surface methodology for multi-objective optimization of fly ash-GGBS based geopolymer mortar. *Constr Build Mater* 2022;315:125644. <https://doi.org/10.1016/j.conbuildmat.2021.125644>
- [3] Chen C, Shenoy S, Li L, Tian Q, Zhang H. Preparation of one-part geopolymers using coal gasification slag: Effect of alkali fusion product additive and liquid/solid ratio. *Journal of Industrial and Engineering Chemistry* 2024;137:207-15. <https://doi.org/10.1016/j.jiec.2024.03.006>
- [4] Shi C, Jiménez AF, Palomo A. New cements for the 21st century: The pursuit of an alternative to Portland cement. *Cem Concr Res* 2011;41:750-63. <https://doi.org/10.1016/j.cemconres.2011.03.016>
- [5] Liew YM, Kamarudin H, Mustafa Al Bakri AM, Bnhussain M, Luqman M, Khairul Nizar I, et al. Optimization of solids-to-liquid and alkali activator ratios of calcined kaolin geopolymeric powder. *Constr Build Mater* 2012;37:440-51. <https://doi.org/10.1016/j.conbuildmat.2012.07.075>
- [6] Xu H, van Deventer JSJ, Lukey GC. Effect of Alkali Metals on the Preferential Geopolymerization of Stilbite/Kaolinite Mixtures. *Ind Eng Chem Res* 2001;40:3749-56. <https://doi.org/10.1021/ie010042b>
- [7] Somna K, Jaturapitakkul C, Kajitvichyanukul P, Chindaprasirt P. NaOH-activated ground fly ash geopolymer cured at ambient temperature. *Fuel* 2011;90:2118-24. <https://doi.org/10.1016/j.fuel.2011.01.018>
- [8] Phair JW, Van Deventer JSJ. Effect of silicate activator pH on the leaching and material characteristics of waste-based inorganic polymers. *Miner Eng* 2001;14:289-304. [https://doi.org/10.1016/S0892-6875\(01\)00002-4](https://doi.org/10.1016/S0892-6875(01)00002-4)
- [9] Yao X, Zhang Z, Zhu H, Chen Y. Geopolymerization process of alkali-metakaolinite characterized by isothermal calorimetry. *Thermochim Acta* 2009;493:49-54. <https://doi.org/10.1016/j.tca.2009.04.002>
- [10] Zuhua Z, Xiao Y, Huajun Z, Yue C. Role of water in the synthesis of calcined kaolin-based geopolymer. *Appl Clay Sci* 2009;43:218-23. <https://doi.org/10.1016/j.clay.2008.09.003>
- [11] Provis JL, Duxson P, Lukey GC, Separovic F, Kriven WM, van Deventer JSJ. Modeling Speciation in Highly Concentrated Alkaline Silicate Solutions. *Ind Eng Chem Res* 2005;44:8899-908. <https://doi.org/10.1021/ie050700i>
- [12] Jaya NA, Liew YM, Heah CY, Abdullah MMAB. Effect of solid-to-liquid ratios on metakaolin geopolymers, 2018, p. 020099. <https://doi.org/10.1063/1.5080912>
- [13] Mohammed ASSK, Géber R. Effect of liquid-solid ratio on metakaolin-based geopolymer binder properties. *Pollack Periodica* 2024. <https://doi.org/10.1556/606.2024.01141>
- [14] Ibrahim M, Wan Ibrahim WM, Al Bakri Abdullah MM, Sauffi AS, Vizureanu P. Effect of Solid-To-Liquids and Na<sub>2</sub>SiO<sub>3</sub>-To-NaOH Ratio on Metakaolin Membrane Geopolymers. *Archives of Metallurgy and Materials* 2021:695-702. <https://doi.org/10.24425/amm.2022.137808>
- [15] Nur AJ, Liew YM, Al Bakri AMM, Heah CY. Thermophysical Properties of Metakaolin Geopolymers Based on Na<sub>2</sub>SiO<sub>3</sub>/NaOH Ratio. *Solid State Phenomena* 2018;280:487-93. <https://doi.org/10.4028/www.scientific.net/SSP.280.487>
- [16] Wang H, Li H, Yan F. Synthesis and mechanical properties of metakaolinite-based geopolymer. *Colloids Surf A Physicochem Eng Asp* 2005;268:1-6. <https://doi.org/10.1016/j.colsurfa.2005.01.016>

- [17] Pacheco-Torgal F, Castro-Gomes J, Jalali S. Alkali-activated binders: A review. Part 2. About materials and binders manufacture. *Constr Build Mater* 2008;22:1315-22. <https://doi.org/10.1016/j.conbuildmat.2007.03.019>
- [18] Nikoloutsopoulos N, Sotiropoulou A, Kakali G, Tsivilis S. The effect of Solid/Liquid ratio on setting time, workability and compressive strength of fly ash based geopolymers. *Mater Today Proc* 2018;5:27441-5. <https://doi.org/10.1016/j.matpr.2018.09.062>
- [19] Sasui S, Kim G, van Riessen A, Lim C, Eu H, Park J, et al. Effects of Na<sub>2</sub>SiO<sub>3</sub>/NaOH ratio in alkali activator on the microstructure, strength and chloride ingress in fly ash and GGBS based alkali activated concrete. *Journal of Building Engineering* 2024;98:111255. <https://doi.org/10.1016/j.jobee.2024.111255>
- [20] Aouan B, Alehyen S, Fadil M, EL Alouani M, Khabbazi A, Atbir A, et al. Compressive strength optimization of metakaolin-based geopolymer by central composite design. *Chemical Data Collections* 2021;31. <https://doi.org/10.1016/j.cdc.2020.100636>
- [21] Davidovits J. *Geopolymer Chemistry and Applications* 5th ed. 2020.
- [22] Zibouche F, Kerdjoudj H, de Lacaille J-B d'Espinose, Van Damme H. Geopolymers from Algerian metakaolin. Influence of secondary minerals. *Appl Clay Sci* 2009;43:453-8. <https://doi.org/10.1016/j.clay.2008.11.001>
- [23] Kong DLY, Sanjayan JG, Sagoe-Crentsil K. Comparative performance of geopolymers made with metakaolin and fly ash after exposure to elevated temperatures. *Cem Concr Res* 2007;37:1583-9. <https://doi.org/10.1016/j.cemconres.2007.08.021>
- [24] Heah CY, Kamarudin H, Mustafa Al Bakri AM, Bnhussain M, Luqman M, Khairul Nizar I, et al. Study on solids-to-liquid and alkaline activator ratios on kaolin-based geopolymers. *Constr Build Mater* 2012;35:912-22. <https://doi.org/10.1016/j.conbuildmat.2012.04.102>
- [25] Bowen F, Jiesheng L, Jing W, Yaohua C, Tongtong Z, Xiaoming T, et al. Investigation on the impact of different activator to solid ratio on properties and micro-structure of metakaolin geopolymer. *Case Studies in Construction Materials* 2022;16:e01127. <https://doi.org/10.1016/j.cscm.2022.e01127>
- [26] Shoaee P, Musaei HR, Mirlohi F, Narimani zamanabadi S, Ameri F, Bahrami N. Waste ceramic powder-based geopolymer mortars: Effect of curing temperature and alkaline solution-to-binder ratio. *Constr Build Mater* 2019;227:116686. <https://doi.org/10.1016/j.conbuildmat.2019.116686>
- [27] Liew YM, Kamarudin H, Mustafa Al Bakri AM, Bnhussain M, Luqman M, Khairul Nizar I, et al. Influence of Solids-to-liquid and Activator Ratios on Calcined Kaolin Cement Powder. *Phys Procedia* 2011;22:312-7. <https://doi.org/10.1016/j.phpro.2011.11.049>
- [28] Jaya NA, Yun-Ming L, Cheng-Yong H, Abdullah MMAB, Hussin K. Correlation between pore structure, compressive strength and thermal conductivity of porous metakaolin geopolymer. *Constr Build Mater* 2020;247:118641. <https://doi.org/10.1016/j.conbuildmat.2020.118641>
- [29] Kwek SY, Awang H, Cheah CB. Influence of Liquid-to-Solid and Alkaline Activator (Sodium Silicate to Sodium Hydroxide) Ratios on Fresh and Hardened Properties of Alkali-Activated Palm Oil Fuel Ash Geopolymer. *Materials* 2021;14:4253. <https://doi.org/10.3390/ma14154253>
- [30] Thokchom S, Ghosh S, Ghosh P. Effect of water absorption, porosity and sorptivity on durability of geopolymer mortars 2009;4.
- [31] Zhou W, Yan C, Duan P, Liu Y, Zhang Z, Qiu X, et al. A comparative study of high- and low-Al<sub>2</sub>O<sub>3</sub> fly ash based-geopolymers: The role of mix proportion factors and curing temperature. *Mater Des* 2016;95:63-74. <https://doi.org/10.1016/j.matdes.2016.01.084>
- [32] Ibrahim M, Megat Johari MA, Rahman MK, Maslehuudin M. Effect of alkaline activators and binder content on the properties of natural pozzolan-based alkali activated concrete. *Constr Build Mater* 2017;147:648-60. <https://doi.org/10.1016/j.conbuildmat.2017.04.163>
- [33] Xie T, Visintin P, Zhao X, Gravina R. Mix design and mechanical properties of geopolymer and alkali activated concrete: Review of the state-of-the-art and the development of a new unified approach. *Constr Build Mater* 2020;256:119380. <https://doi.org/10.1016/j.conbuildmat.2020.119380>
- [34] Hameed AM, Rawdhan RR, Al-Mishhadani SA. Effect of various factors on the manufacturing of geopolymer mortar. *Archives of Science* 2017;1:1-8.
- [35] Xu H, Van Deventer JSJ. The geopolymerisation of alumino-silicate minerals. *Int J Miner Process* 2000;59:247-66. [https://doi.org/10.1016/S0301-7516\(99\)00074-5](https://doi.org/10.1016/S0301-7516(99)00074-5)
- [36] Moutaoukil G, Alehyen S, Sobrados I, Fadil M, Taibi M. Optimization of compressive strength of fly ash-based geopolymers using central composite design. *Bulletin of Materials Science* 2021;44:138. <https://doi.org/10.1007/s12034-021-02424-3>
- [37] Villa C, Pecina ET, Torres R, Gómez L. Geopolymer synthesis using alkaline activation of natural zeolite. *Constr Build Mater* 2010;24:2084-90. <https://doi.org/10.1016/j.conbuildmat.2010.04.052>
- [38] Škvára F, Kopecký L, Nemecek J, Bittnar Z. Microstructure of geopolymer materials based on fly ash. *Ceramics-Silikaty* 2006;50:208-15.



- [39] Al Bakri AMM, Kamarudin H, Bnhussain M, Rafiza AR, Zarina Y. Effect of Na<sub>2</sub>SiO<sub>3</sub>/NaOH ratios and NaOH molarities on compressive strength of fly-ash-based geopolymer. *ACI Mater J* 2012;109:503. <https://doi.org/10.14359/51684080>
- [40] Liew YM, Heah CY, Mohd Mustafa AB, Kamarudin H. Structure and properties of clay-based geopolymer cements: A review. *Prog Mater Sci* 2016;83:595-629. <https://doi.org/10.1016/j.pmatsci.2016.08.002>
- [41] Yong-Sing N, Yun-Ming L, Bakri Abdullah MM Al, Hui-Teng N, Hussin K, Yong HC, et al. Effect of Solid-to-Liquid Ratio on Thin Fly Ash Geopolymer. *IOP Conf Ser Mater Sci Eng* 2020;743:012006. <https://doi.org/10.1088/1757-899X/743/1/012006>
- [42] Kong DLY, Sanjayan JG, Sagoe-Crentsil K. Factors affecting the performance of metakaolin geopolymers exposed to elevated temperatures. *J Mater Sci* 2008;43:824-31. <https://doi.org/10.1007/s10853-007-2205-6>
- [43] Marczyk J, Ziejewska C, Pławecka K, Bąk A, Łach M, Korniejenko K, et al. Optimizing the L/S Ratio in Geopolymers for the Production of Large-Size Elements with 3D Printing Technology. *Materials* 2022;15:3362. <https://doi.org/10.3390/ma15093362>
- [44] Maheswaran M, Christy CF, Muthukannan M, Arunkumar K, Vigneshkumar A. Parametric study on the performance of industrial byproducts based geopolymer concrete blended with rice husk ash & nano silica. *Research on Engineering Structures and Materials* 2023.
- [45] Maheswaran M, Freeda Christy C, Muthukannan M, Arunkumar K, Vigneshkumar A. Parametric Study on Strength Performance of Geopolymer Concrete Using Industrial By-Products, 2024, p. 113-24. [https://doi.org/10.1007/978-981-97-1080-5\\_10](https://doi.org/10.1007/978-981-97-1080-5_10)
- [46] Kong DLY, Sanjayan JG, Sagoe-Crentsil K. Comparative performance of geopolymers made with metakaolin and fly ash after exposure to elevated temperatures. *Cem Concr Res* 2007;37:1583-9. <https://doi.org/10.1016/j.cemconres.2007.08.021>
- [47] Al Bakri Abdullah MM, Kamarudin H, Ismail KN, Bnhussain M, Zarina Y, Rafiza AR. Correlation between Na<sub>2</sub>SiO<sub>3</sub>/NaOH Ratio and Fly Ash/Alkaline Activator Ratio to the Strength of Geopolymer. *Adv Mat Res* 2011;341-342:189-93. <https://doi.org/10.4028/www.scientific.net/AMR.341-342.189>
- [48] Abdullah MMAB, Kamarudin H, Bnhussain M, Ismail KN, Rafiza AR, Zarina Y. The Relationship of NaOH Molarity, Na<sub>2</sub>SiO<sub>3</sub>/NaOH Ratio, Fly Ash/Alkaline Activator Ratio, and Curing Temperature to the Strength of Fly Ash-Based Geopolymer. *Adv Mat Res* 2011;328-330:1475-82. <https://doi.org/10.4028/www.scientific.net/AMR.328-330.1475>
- [49] Shilar FA, Ganachari S V., Patil VB, Khan TMY, Javed S, Baig RU. Optimization of Alkaline Activator on the Strength Properties of Geopolymer Concrete. *Polymers (Basel)* 2022;14:2434. <https://doi.org/10.3390/polym14122434>
- [50] Abu Hashim MF, Ghazali CMR, Daud YM, Faris MA, Al Bakri Abdullah MM, Zainal FF, et al. Mechanical Effects on Different Solid to Liquid Ratio of Geopolymer Filler in Epoxy Resin. *Archives of Metallurgy and Materials* 2021:215-20. <https://doi.org/10.24425/amm.2022.137492>
- [51] Longhi MA, Rodríguez ED, Walkley B, Zhang Z, Kirchheim AP. Metakaolin-based geopolymers: Relation between formulation, physicochemical properties and efflorescence formation. *Compos B Eng* 2020;182:107671. <https://doi.org/10.1016/j.compositesb.2019.107671>
- [52] Gharzouni A, Ouamara L, Sobrados I, Rossignol S. Alkali-activated materials from different aluminosilicate sources: Effect of aluminum and calcium availability. *J Non Cryst Solids* 2018;484:14-25. <https://doi.org/10.1016/j.jnoncrysol.2018.01.014>
- [53] Pnias D, Giannopoulou IP, Perraki T. Effect of synthesis parameters on the mechanical properties of fly ash-based geopolymers. *Colloids Surf A Physicochem Eng Asp* 2007;301:246-54. <https://doi.org/10.1016/j.colsurfa.2006.12.064>
- [54] Merabtene M, Kacimi L, Clastres P. Elaboration of geopolymer binders from poor kaolin and dam sludge waste. *Heliyon* 2019;5:e01938. <https://doi.org/10.1016/j.heliyon.2019.e01938>